

Soft Foot Sensor Design and Terrain Classification for Dynamic Legged Locomotion

Xiaofeng Guo¹, Bryan Blaise², Jennifer Molnar², Jeremiah Coholich¹, Shantanu Padte¹,
Ye Zhao^{1*}, and Frank L. Hammond III^{2*}

Abstract—Dynamic legged locomotion is being explored as a means to maneuver on rugged and unstructured terrains. However, limited foot contact sensing capabilities often prohibit bipedal robots from being deployed on complex terrains. Locomotion over cluttered outdoor environments requires the contacting foot to be aware of terrain geometries, stiffness, and granular media properties. To achieve this, we designed a new soft contact pad integrated with a variety of embedded sensors, including tactile, acoustic, capacitive, and temperature sensors, as well as an accelerometer. In addition, we devised a terrain classification algorithm based on features extracted from those sensors and various real-world terrains. The classifier uses these features as inputs and classifies various terrains via Random Forests and a memory function. Our cross-validation tests demonstrate that the proposed classification algorithm achieves an accuracy of about 96.5%, manifesting the applicability of this foot sensing device to bipedal locomotion over diverse terrains.

I. INTRODUCTION

Legged robots are able to traverse diverse, complex, and unstructured terrain, which is often required to execute hazardous or burdensome tasks in the field. However, state-of-the-art control methods for dynamic locomotion primarily focus on a single terrain – for instance, level concrete – with a few exceptions that include soft terrain locomotion [1], [2], [3]. In that regard, the development of a unified locomotion control strategy capable of adroitly traversing a wide variety of unstructured terrains has yet to be explored, let alone a controller for coping with emergency situations such as foot slipping and sinking. One cause of this is the lack of rich contact sensing information to capture terrain features, including contact patch area, friction properties, stiffness, and terrain moisture. Information-rich, robust, and compliant contact foot sensing is necessary to design contact-aware planning and control strategies for dynamic locomotion over austere terrains.

Dynamic locomotion over austere terrains is gaining increasing attention in the field of field robotics and animal locomotion [4]. The work of [5] provided a stability criterion to allow model-based control methods to function on homogeneous, deformable terrain. The study of [6]

²B. Blaise, J. Molnar, and F. Hammond are with the George W. Woodruff School of Mechanical Engineering and the Wallace H. Coulter Department of Biomedical Engineering, Georgia Institute of Technology, Atlanta, GA 30332, USA {bblaise3, jmolnar6, fhammond3}@gatech.edu.

¹X. Guo, J. Coholich, S. Padte, and Y. Zhao are with the Laboratory for Intelligent Decision and Autonomous Robots in the George W. Woodruff School of Mechanical Engineering, Georgia Institute of Technology, Atlanta, GA 30332, USA {xguo335, jcuholich, spadte6, yzhao301}@gatech.edu. *co-corresponding authors.

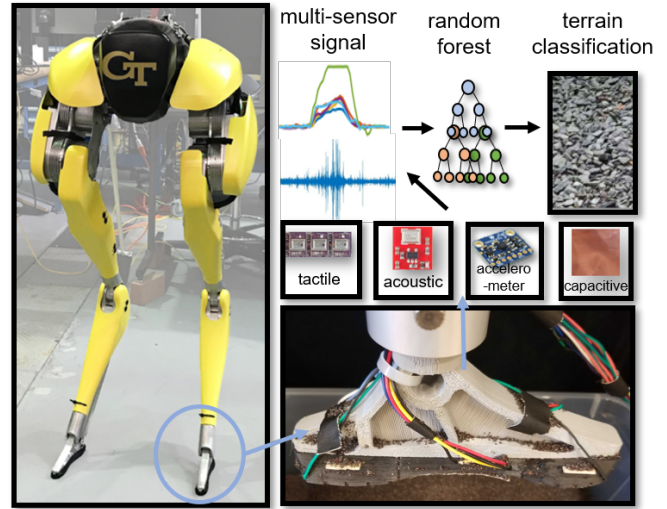


Fig. 1. Our work focuses on the development of a soft, sensor-embedded foot for legged robots. Signals from haptic, acoustic, capacitive sensors and an accelerometer are used for terrain classification.

presented a model for granular terrain with an approach to motion planning for maneuvering in such terrain. In addition, the authors in [7] introduce a method to estimate the ground normal force for mitigating the risk of slippage, which is more likely on deformable terrain. Rebula et. al. [8] developed a controller for a quadruped robot walking on known rough terrain that could react to unmodeled foot slippage and impassable terrain. Grizzle et. al. have achieved bipedal robot walking with a Cassie robot on a set of terrains that includes sand, snow, and grass [2]. However, this remarkable mobility primarily relies on the robustness of low-level joint controllers, without explicitly incorporating terrain information into planning and control strategies. In general, there is still a long way to go towards enabling legged robots to walk robustly and elegantly over a variety of rough terrains. To take one step towards this goal, this study proposes to design a rich contact sensing pad embedded with various sensors and accurate classification algorithms for rough terrain identification, which is still missing for a majority of current bipedal robots.

In contrast to robots, humans use multiple sources of sensory input to identify terrain, including tactile, auditory, and visual feedback. To mimic this and allow legged robots to identify terrain, we design a multi-sensory system on the soft sole of a Cassie-style foot, with the eventual goal of installation on a Cassie robot. Features extracted from the data are input into a novel terrain classification algorithm,

which consists of an implementation of Random Forests with a memory function. Fig.1 depicts the integration of our sensing foot into the Cassie robot.

To the best of the authors' knowledge, this study takes the first step towards integrating an array of different terrain sensors for accurate terrain classification and frictional contact estimation. This line of research paves the way for future creation of terrain-aware locomotion planning and control. The contribution of this study is three-fold: (i) A soft contact sensor pad for a Cassie bipedal robot with a compact and sophisticated contact sensing system; (ii) A terrain classification algorithm achieving high-accuracy classification performance for ten types of real-world terrains; (iii) Experimental evaluations and performance benchmarking of diverse terrain sensing tests and robustness to sensor failures.

II. RELATED WORK

Terrain classification is significant for wheeled and legged robot locomotion over complex terrain. Although numerous existing works employ vision methods via on-board cameras and run surface texture recognition algorithms [9], classification methods based on up-to-date sensing sources attract increasing attention in the field [1], [10]. A novel approach uses data from acoustic sensors mounted on the robot, operating immune to lighting conditions or visual obfuscation, which often causes failures of vision methods. Libby and Stentz [11] solely relied on acoustic data while Christie and Kottege [3] added a noise removal method to filter out servo noise. Another method proposed by Giguere et. al. made use of a tactile probe dragged along the ground, using only accelerometer data to classify between ten types of terrains [12], [13]. Others have used contact wrench data from a 6-axis load cell to classify terrain [14], or alternatively sensed the distribution of contact forces with a sensor array [15], [16]. Although simple sensing solutions likely have better computational efficiency and achieve moderate accuracy, high-resolution and accurate terrain sensors for diverse terrains have not yet emerged.

Integrating multifarious sensors generally yields more capable terrain classification, with the most common sensor combinations consisting of proprioceptive sensors that already exist on most robots. These typically include inertial measurement units (IMUs), joint encoders, and motor current sensors. Kolvenbach et al. [17] used a force/torque sensor and IMU to gather impact data and classified nine different variations of Martian soil with 98% accuracy. Giguere et al. [18] performed experiments with an amphibious RHex robot and achieved 90% accuracy in identifying six different terrains using via an IMU, motor position and current. Similarly, [19] only used IMU data and motor state for a millirobotic crawler. Degrave et al [20] did the same for the Puppy II robot, but added tactile sensors to each foot. Walas used vision, depth, and tactile sensors to achieve an accuracy of 94% over twelve types of terrains [1]. Halatci et al [21] also combined vision and tactile data to differentiate between Martian rock, sand, and mixed rock and sand. Compared to the methods above, our sensor pad focuses

on integrating multi-source sensing information, including auditory and haptic signals. In particular, our study is one of the first to integrate auditory and tactile signals and employ memory functions in a terrain classification algorithm.

A variety of classification and learning methods, primarily supervised ones, have been employed for terrain classification. The most popular approach is to train a Support Vector Machine (SVM) to discriminate between different terrain types [9], [11], [3], [15], [19], [1] and more. Degrave et. al. [20] experimented with different learning methods, including unsupervised methods, and found that only linear regression performed poorly (due to nonlinearities) and reservoir computing was best. [12], [13], studies using only one sensor, were able to achieve a high accuracy by training a simple artificial neural network.

Our work integrates five types of sensors, as shown in Fig. 2. To the best of the authors' knowledge, this sensing system will offer a legged robot richer terrain-sensing capabilities than any previous approaches. Additionally, we believe no previous approach has incorporated the use of an acoustic sensor together with many other sensors for terrain classification. It is worthwhile to mention that, unlike the fields of computer vision or natural language processing, there are no open-source datasets to benchmark terrain classification algorithms, so performance comparisons among different approaches are not our objective. Instead, we will demonstrate that the proposed sensor pad offers a high accuracy of terrain classification and robustness to sensor failures.

III. DESIGN OF CONTACT SENSING PAD

Soft materials, which are mechanically deformable, are often used in situations where their compliance adds to the robustness, adaptability, and simplicity of a structure. In this case, a stiff but deformable rubber (Smooth-Sil 960, Smooth-On, Inc.) was used to hold five types of sensors in place on the model foot: two TakkStrip2 pressure sensors, an acoustic sensor, a capacitive sensor, a temperature sensor, and an accelerometer. For practical inclusion on a Cassie robot, the foot was built to match the standard Cassie foot's shape, with the sensors embedded in the rubber sole or attached to the side of the foot. (See Fig. 2.)

The stiffness of the elastomer supported and dispersed the heavy pressures experienced by the foot during testing, protecting the embedded elements, while also naturally deforming to allow key sensors close access to the terrains' surface. The elastomeric foot material was also used to tune the pressure sensitivity of the TakkStrip2 pressure sensor: varying the depth of the sensors within the foot affected whether pressures were sensitive to local or dispersed forces.

The tactile sensors, TakkStrip2 (Righthand Robotics, Inc.), are an array of six barometric pressure sensors (MPL115A2), each encapsulated with an elastomeric pad to transduce contact pressure into environmental pressure. The force range of each subsensor is about 2N, but by encapsulating the TakkStrip2 inside the rubber of the soft contact pad, the contact forces are dispersed over a larger area and the TakkStrip2's force range is enlarged. The TakkStrip2s

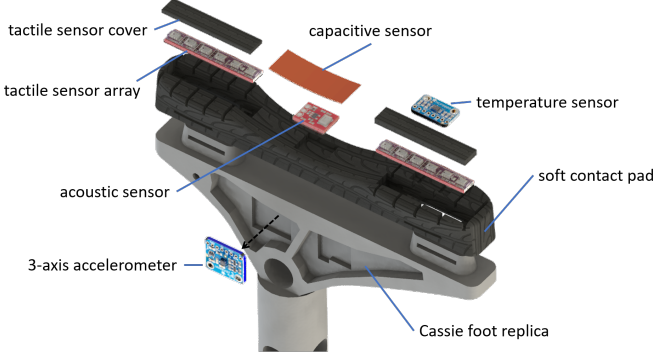


Fig. 2. Exploded view of the sensor-embedded Cassie foot design.

were embedded at a depth that provided a force range of approximately 10–250N. One TakkStrip2 was embedded in the front of the foot, and one in the heel. A temperature sensor (MCP9808, Microchip Technology, Inc.) was embedded in the elastomer next to the heel TakkStrip2, with its temperature-sensing element exposed. Wiring was routed between the treads of the foot to allow even contact of the sensorized sole with the terrain. While the current pad prototype integrates all of aforementioned sensors, the front tactile sensor and the temperature sensor are not used for classification in this work. They will be used for comprehensive terrain sensing in the future work.

The capacitive and acoustic sensors (ADMP401, Analog Devices, Inc.) were incorporated into the arched segment of the sole, while an accelerometer (MMA8451, Adafruit Industries LLC) was affixed to the rigid top of the foot. The acoustic sensor was positioned in the arch of the foot, facing downward to shield it from ambient noise. It was protected from physical contact with the terrain by a piece of conductive copper tape, 20mm × 55mm. This also functioned as the major component of the capacitive sensing circuit, with the copper tape attached to the V_{DD} side of a $1.8\text{M}\Omega$ resistor connected between 3.3V power and ground. The V_{DD} voltage was sourced from an I/O pin on a 32-bit MSP432 microcontroller (Texas Instruments Inc.) and repeatedly charged and discharged. The capacitance of the copper tape changed with proximity to moisture and other dielectrics, which affected discharge time as measured by a NI-DAQ (National Instruments, Inc.).

The accelerometer, temperature, and tactile sensors are connected to the MSP432 microcontroller via I2C communication protocol. The maximum frequency at which all sensors could be read sequentially was 38Hz. The acoustic and capacitive sensors were measured via the analog input ports of the NI-DAQ (National Instruments, Inc.) at 22kHz (although the capacitor was charged via the MSP432).

The soft contact pad was cast in three sections from SmoothSil 960 (Smooth-On, Inc.) colored black with Silc Pig pigment (Smooth-On, Inc.). They were fastened to the 3D-printed PLA frame of the foot via wooden connectors and glued together with Sil-Poxy (Smooth-On, Inc.).

TABLE I
NUMBER OF FEATURES FOR DIFFERENT SENSORS

sensor type	number of features
tactile sensor	45
acoustic sensor	7
accelerometer	18
capacitive sensor	11
all	81

IV. TERRAIN CLASSIFICATION

This section describes our data processing procedure and classification algorithms. Details on feature extraction are elaborated based on various terrain sensing signals.

A. Signal processing for data acquisition

A multi-sensor continuous-time series was acquired from the testbed described in the next section. A preprocessing and segmentation process (Fig. 3) transformed each impact into one data point.

1) *Signal pre-processing*: Raw data from the sensors are noisy and require signal preprocessing to increase the signal-noise ratio and preserve useful terrain information. Even post-calibration, there is linear zero drift in the haptic signal which can be removed with a detrending function. The acoustic signal is preprocessed with a high-pass filter and spectrum subtraction strategy to filter out ambient noise from the Instron machine used in tests. Acceleration and capacitive signals are put through zero alignment for post processing.

2) *Time series segmentation*: The continuous sensor signals are segmented into discrete periods, or data points, each corresponding to the contact experienced during one step. Each data point also includes about 0.5 sec of data from the non-contacting period before and after each impact for better classification. The segmentation is comprehensively conducted on all sensor signals, making it viable even when certain signals are information-poor. For example, if the terrain is so uneven that initial contact does not produce pressure over the embedded tactile sensor, it is difficult to segment sensor signals using tactile sensor data due to lack of information. Additionally, the acoustic signal – which is heavily affected by environmental noise – only records useful information during impact. By appropriately segmenting the data, we can easily distinguish between noise and contact information. The spectrum subtraction then reduces noise during the contact period by subtracting out what was recorded the remainder of the time.

B. Feature extraction

This subsection introduces the features that are extracted from each sensor signal for classification. Although the nearest neighbors with Dynamic Time Wrapping (DTW) works well for many applications in time series classification and [22] demonstrated that the DTW distance can be used as a feature, this algorithm performs poorly in our experiments. Due to different sampling frequencies among sensors and variations in the segmenting process, each segment of time-series data contains a different number of data points. To

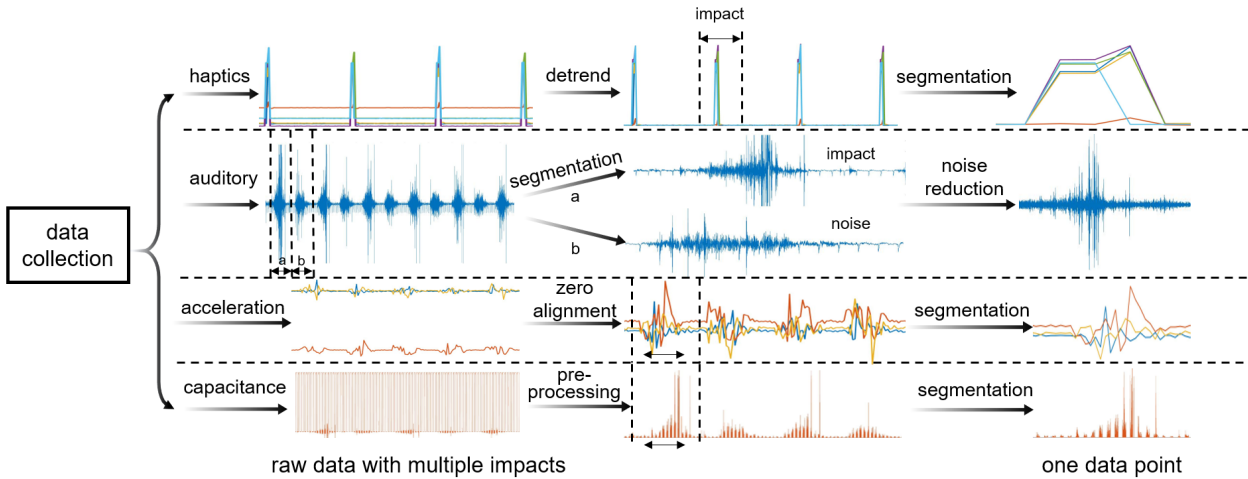


Fig. 3. Signal processing for data acquisition. After collecting raw data for multiple foot impacts, signal pre-processing and segmentation are used to convert it into a set of data points for feature extraction in Section IV-B. All sub-figures represent curves of signal value versus time.

maintain the same dimension for the classification algorithm, we extracted 81 features in total to represent the signals, as shown in Table I and Fig. 4. Since the haptic sensors and accelerometer have a 38Hz sampling frequency and the acoustic and capacitive sensors have a 22kHz sampling frequency, we handle the first two signals only in the time domain while the other two in both time and frequency domains. In total, there are 81 features described here.

1) Haptic signal: We use the force distribution of six-point-array tactile signal and multiple statistical measurements, where each point includes maximum value, minimum value, the value when the sum value of the six points reaches its peak, and the first to the fourth standardized moment of each signal. We also use the maximum value and minimum value of the sum value as well as define the time to reach 80% of its maximum value, a possible indication of the terrain stiffness. There are in total $6 \times 7 + 3 = 45$ features.

2) Acoustic signal: In the time domain, the Zero-Crossing Rate (ZCR), the rate of signal sign changes (i.e. zero-crossing), is used as one feature. ZCR is a common feature used in auditory classification and is demonstrated to be effective in speech processing. A fixed number of Fast Fourier Transform (FFT) is used to obtain the frequency spectrum of each signal, ensuring frequency spectra of the same dimension despite different lengths in the time domain.

Inspired by Mine's work [23], we define the sum of amplitudes in each frequency band as the spectral band energy and use it as a feature. Specifically, the acoustic signal frequency is between 4 kHz and 17 kHz after noise reduction. We set 4096 Hz as one frequency band and each one has an overlapping frequency of 2048 Hz with its neighbor frequency band. Therefore, seven features (six spectral band energies and one ZCR) are extracted as features.

3) Acceleration: For 3-axis linear acceleration, we use the ZCR of the first-order derivative of the raw data of each axis to represent the signal fluctuation frequency. Statistical measurements including the maximum value, minimum value,

sum, mean, and variance for each axis acceleration are also extracted as features ($3 \times 6 = 18$ features in total).

4) Capacitive signal: We use the same frequency band technique for the capacitive sensor as we did for the acoustic sensor, but enlarge the whole frequency range to 0 Hz to 22 kHz. We extract multiple features in time domain, such as mean and variance, and frequency domain, such as spectral band energy ($2 + 9 = 11$ features in total).

C. Classification algorithm

This section describes the high-accuracy classification algorithm developed for use on various terrain conditions. We use Random Forests as our basic classifier and employ a memory function to factor in the relationship between consecutive periods to improve the classification performance.

The classification procedure is to predict the terrain category via a training data set with terrain labels. The Random Forests (RFs) is a classification algorithm combining a multitude of tree predictors, each of which depends on the values of a randomly sampled vector. All the trees in the same forest use the same distribution. Every tree casts a unit vote for the final classification result [24]. The whole forest takes the number of votes received by each class to represent the predicted probability of that class and uses the class with the maximum predicted probability as the final predicted class. Additionally, the most important parameter of RFs is the number of trees. Increasing this number increases accuracy at the expense of efficiency. According to this, we set the number of trees to be 100 in our experiment.

Although the continuous-time series is segmented into multiple data points, certain relationships still exist among them and are explored in our study to provide more information to the classification algorithm. In practical scenarios, a legged robot will likely take multiple steps on one terrain before switching to another one. Therefore, it is reasonable that the $(k+1)^{\text{th}}$ step classification incorporates the k^{th} step result. Accordingly, a memory function f is designed. We denote s as the final predicted probability and $p_{k,i}$ as the

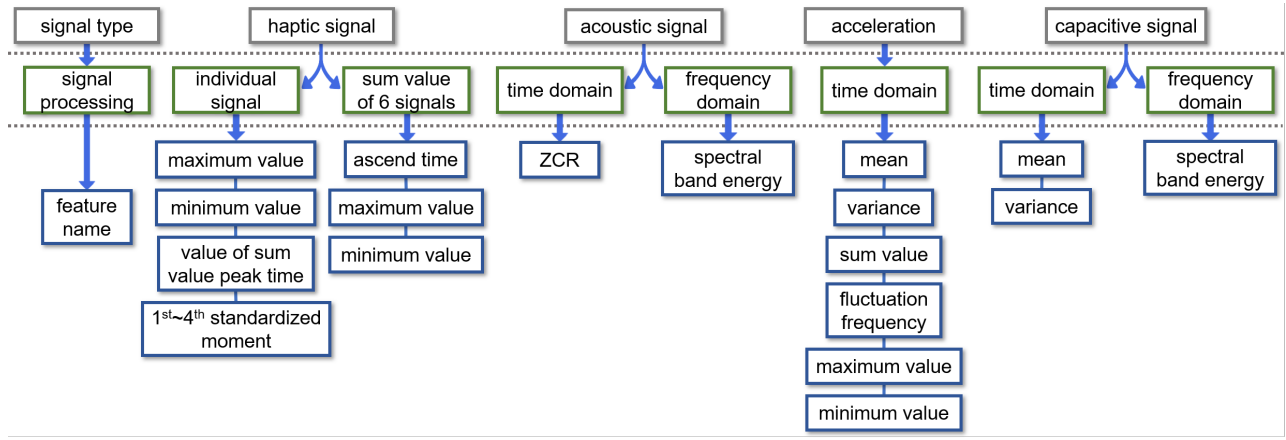


Fig. 4. Diagram of 81 features extracted from sensor signal of every data point after signal processing such as FFT.

predicted probability of i^{th} terrain output by Random Forests at the k^{th} period. Hence, we have $s_{k+1,i} = f(s_{k,i}, p_{k,i})$. For problem simplicity, we choose a linear combination of member functions of $s_{k,i}$ and $p_{k,i}$, i.e., $f(s_{k,i}, p_{k,i}) = f_1(s_{k,i}) + f_2(p_{k,i})$. A performance comparison among various memory functions is conducted in the next section.

V. EXPERIMENTAL RESULTS

A. Experiment setup

To produce a controlled environment for simulating the stepping pattern of the Cassie robot, we conducted a cyclic impact test on an Instron 5965 machine. In a single cycle, the sensorized foot moves downward at 50mm/s to a peak force of 250N, pauses for 0.5 sec, returns to the initial position at 50mm/s, and then pauses for another 0.5 sec. Tests were organized into 4 sets of 25 cycles on each of 10 different terrains, with the terrain being shifted or perturbed between sets to introduce natural variation. Five of these trials were conducted per terrain, to provide both training and testing data, for a total of 5000 data points across the 10 terrains. The terrains were chosen to simulate both indoor and outdoor terrain environments and included: a wood board (WB), foam mat (FM), gravel (GR), rug (RU), metal plate (MP), concrete block (CB), dry pine straw mulch (DM), wet pine straw mulch (WM), dry poppy seeds (DP), and wet poppy seeds (WP), as shown in Fig. 5. Terrains such as poppy seeds and gravel were contained within a plastic box and manually raked smooth between cycles. The test set-up is shown in Fig. 6.

Next, terrain classification tests based on the collected data set are conducted to demonstrate the performance of our terrain classification algorithm.

B. Cross-validation test

Since data points within the same impact trial are highly repeatable, running cross-validation directly on the whole data set will result in an extremely high accuracy. Therefore, we change the cross-validation test to a more difficult scenario by treating one trial as a whole. The whole data set with 200 trials is randomly divided into a training set with

all the data of 160 trials and a test set with the remaining data. The resulting testing and training data sets are used to train and evaluate the model. The whole process is called one test process. In total, 100 test processes are run for every classification algorithm. Next, we will compare the



Fig. 5. Terrain types studied in the classification

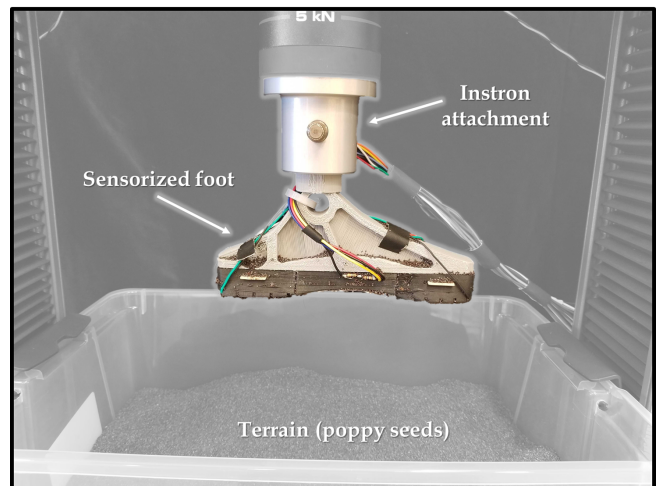


Fig. 6. Experimental test bed, consisting of an Instron-mounted foot, impact cyclically onto various types of terrain. The cyclic foot motion simulates the stepping process of our Cassie Robot.

TABLE II
ACCURACY OF VARIOUS CLASSIFICATION ALGORITHMS

classifiers	average accuracy
KNN	85.7%
RFs	96.2%
NB	78.8%
SVM	87.5%
RFs+MF	96.5%

performance of various classification algorithms.

1) *Accuracy comparison of various classification algorithms:* We propose a terrain classification algorithm based on a combination of Random Forests and memory functions (RFs+MF). We compare its accuracy to that of multiple well-known algorithms including: (i) Naive Bayes (NB), a classifier based on Bayes' theorem; (ii) Support Vector Machine (SVM), a common classifier using a hyper-plane for classification; (iii) K-nearest neighbours algorithm (KNN), a lazy method that finds k nearest data points in the training set for classification; (iv) Random Forests (RFs), a classifier based on multiple decision trees. We use the classifiers in the Matlab toolbox to run tests for NB, KNN, and RFs and use libsvm [25] for SVM. The KNN we use sets the number of nearest data points to be 1, and the tree number of RFs to be 100, which shows the best performance for these classifiers.

The average accuracy of various classifiers are shown in Table II, and the results indicate that our proposed RFs+MF algorithm has the highest accuracy. The confusion matrix (i.e., an error matrix showing the detailed classification performance) for our classification algorithm is shown in Fig. 7. The accuracy for most of the terrains is high, while gravel and dry pin straw mulch have a low accuracy since these unstructured terrains have similar contact force distribution, resulting in similar haptic signals. Meanwhile, there is a large variation among data points of these two terrains, which also increases the difficulty of classification. Additionally, the rug terrain is prone to be misclassified due to the small sound induced by rug impact, compared to the sound induced by impact with the ground locating under the rug.

2) Accuracy comparison of various memory functions:

This subsection evaluates the performance of the proposed classifiers which combine RFs with different memory functions. In our case, the test point indices are designed as a discrete-time sequence. We set memory functions f_1 and f_2 to have the same function structure and compare the results of using linear, polynomial, and exponential functions, as shown in Fig. 8.

According to the cross-validation test results, the Random Forests can output a maximum predicted possibility to the correct class (i.e., correct classification) for most test points, while producing a fairly low correct predicted possibility only at certain discrete test points that result in misclassification. In the case of unchanged terrain, using a memory function enables the previous test points that have high predictability to compensate for those misclassification-prone points (see Fig. 8). This capability is enabled by increasing the predicted possibility of their correct classes. Therefore,

the average classification accuracy increases. The exponential one performs best among all the function structures because the weight of high predicted possibility is enlarged automatically. This exponential one used as the memory function is set to $s_{k+1,i} = e^{3s_{k,i}} + e^{8p_{k+1,i}}$. However, when the terrain changes, the inclusion of a memory function will reduce the predicted possibility for the correct class because previous test points provide a different terrain type than the current one. As a result, when the terrain changes more frequently, the accuracy of the algorithm combined with the memory function will decrease. We compare the performance of the classification algorithm under the following conditions: (i) with Random Forests only, and (ii) with RFs and a memory function under the different frequencies of terrain variations. The result in Fig. 9 shows when the terrain type varies less than 340 times every 1000 test points (i.e., around 3 steps per terrain), the addition of a memory function is beneficial.

3) *Accuracy comparison of various sensor combinations:* In this study, we demonstrate that using all sensor features renders a higher accuracy for all the ten terrains than that of the model using features of an individual or a subset of sensors. In real-world scenarios, sensor failure or breakage occurs frequently, especially when deployed on rugged terrain. By running tests for various sensor combinations, we observe that the accuracy declines but still remains over 93% (see Table III). This shows the robustness to sensor failures. Namely, if one sensor breaks, we can still use the remaining sensors with a model trained on the remaining sensor combination and obtain an accurate result.

4) *Robustness evaluation:* Sensors for terrain classification are prone to break due to intermittent impact with the ground. Although we can design a mechanism to switch the trained model when certain sensors are broken, it is often challenging to detect whether a sensor malfunctions. It is important to evaluate the robustness of the proposed terrain classification model when certain sensors work abnormally. To evaluate this, we manually generate a set of corrupted test points by replacing parts of the sensor signals with noise

		correct class									
		WB	FM	GR	RU	MP	CB	DM	WM	DP	WP
predicted class	WB	95.8%	0.1%	0.0%	6.1%	0.0%	0.2%	0.0%	0.0%	0.0%	0.0%
	FM	0.0%	99.1%	0.1%	3.8%	0.0%	0.0%	0.0%	0.0%	0.0%	0.0%
	GR	0.0%	0.0%	91.5%	0.2%	0.0%	0.0%	4.3%	1.0%	0.0%	0.0%
	RU	2.4%	0.9%	0.9%	86.7%	0.0%	0.0%	0.0%	0.0%	0.0%	0.0%
	MP	0.9%	0.0%	0.0%	0.2%	100.0%	0.0%	0.0%	0.0%	0.0%	0.0%
	CB	0.0%	0.0%	0.0%	0.3%	0.0%	99.8%	1.0%	0.0%	0.0%	0.0%
	DM	0.9%	0.0%	6.8%	2.6%	0.0%	0.1%	93.4%	0.0%	0.0%	0.0%
	WM	0.0%	0.0%	0.2%	0.0%	0.0%	0.0%	0.3%	99.0%	0.0%	0.0%
	DP	0.0%	0.0%	0.0%	0.0%	0.0%	0.0%	1.0%	0.0%	100.0%	0.0%
	WP	0.0%	0.0%	0.4%	0.0%	0.0%	0.0%	0.0%	0.0%	0.0%	100.0%

Fig. 7. Results of our classification algorithm based on multi-sensor signals. The number in each cell represents the percentage of prediction for each case and the diagonal number shows the correctly predicted cases.

TABLE III
COMPARISON OF CLASSIFICATION ACCURACY OF VARIOUS SENSOR COMBINATIONS

classification accuracy (%) sensors	terrain type	WB	FM	GR	RU	MP	CB	DM	WM	DP	WP	Average
		94.5	98.7	82.8	81.6	99.0	98.8	46.6	76.7	97.2	100	87.6
tactile sensor		88.5	71.0	78.7	62.9	79.9	96.6	70.0	91.4	88.8	96.1	82.4
acoustic sensor		79.3	81.7	92.8	76.7	95.2	99.4	88.6	99.0	96.9	99.9	91.0
accelerometer		82.2	73.7	70.2	76.8	88.8	90.3	47.0	93.2	99.4	99.3	82.1
capacitive sensor		95.5	99.0	90.3	83.6	99.9	99.8	89.1	97.5	99.0	100.0	95.4
tactile + acoustic + accelerometer sensors		95.5	99.5	83.4	84.2	99.8	99.8	84.9	93.7	97.8	100.0	93.8
tactile + acoustic + capacitive sensors		95.3	99.3	87.6	88.6	99.9	99.8	93.2	99.0	99.9	99.9	96.3
tactile + accelerometer + capacitive sensors		93.1	93.1	96.7	80.7	99.0	98.8	93.7	99.8	96.7	100.0	95.2
acoustic + accelerometer + capacitive sensors		95.8	99.1	91.5	86.7	100.0	99.8	93.4	99.0	100.0	100.0	96.5
all sensors												

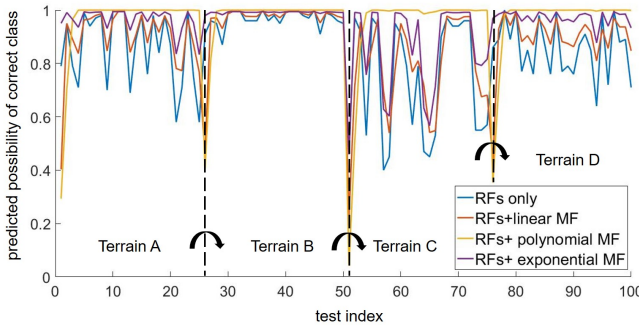


Fig. 8. Comparison of the predicted possibility of correct class among different memory functions.

signals to simulate the abnormal working condition. Gaussian white noise, zero signal, or a combination of the two are used as three types of noise in our work. These corrupted test points are combined with original test points to compose the whole test data set. Fig. 10 demonstrates a high accuracy of our model when tested with various ratios of normal and corrupted data points. The results show the robustness of our model: even when all the data points are corrupted (i.e., the ratio is 0), the classification accuracy is still around 83%. The accuracy increases as the ratio increases as expected.

5) *Discussion:* The cross-validation experiment shows our classification algorithm is accurate when dealing with multi-sensor data. The average accuracy is about 96.5%. In addition, we have employed Principal Component Analysis (PCA) to extract the significant feature dimension and the dimension can be reduced to 18 with an accuracy over 94%,

indicating the potential of our algorithm for faster and real-time deployment. Furthermore, the classification shows an extremely high accuracy as above 98.5% on six types of terrains, while the results of other terrains are also fairly high. Even for the worst identification – the rug terrain, the accuracy is still above 86%.

C. Initial tests under unpredictable impact conditions

To take an initial step towards deploying our sensor pad and classification algorithm for real-world terrain, we explore methods to randomize our data points further and remove the predictability of the Instron machine. In a series of high-variance tests, we remove the integrated foot from the Instron machine and strike the terrain manually. The terrain is struck at different locations for each data point, and the foot is held down for approximately half a second. However, the force of the impact, no longer being set by the Instron, is determined by each experimenter and renders large variations. Additional unpredictability comes in the form of contact angle, speed, and impact duration. In total, 1700 data points of all terrains are collected. We select 1400 points randomly as the training data set and the remaining 300 points as one test data set. By executing 100 test processes, the average classification accuracy of our algorithm is about 89%. Although it is lower than the 96.5% accuracy in the Instron test, the result still validates the real-world deployment capability of our sensor pad and classification algorithms.

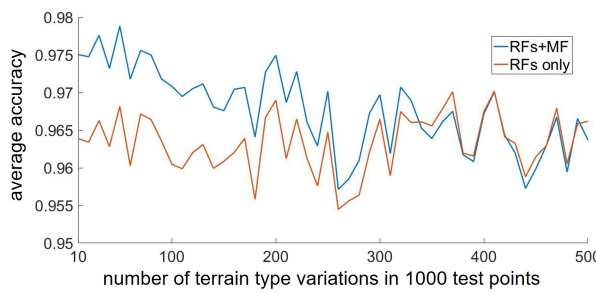


Fig. 9. Comparison of average accuracy between the Random Forests algorithm with and without a memory function about the number of terrain variation.

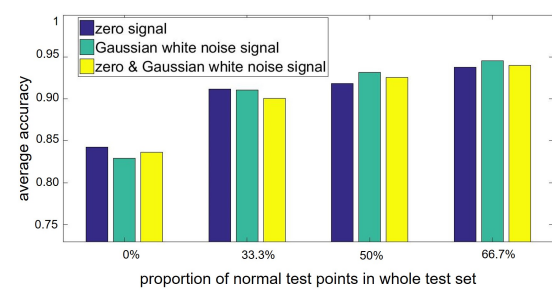


Fig. 10. Average accuracy of our classification algorithm with the mix of different proportions of normal test points and corrupted test points that use different types of signals as the invalid signal.

VI. CONCLUSIONS AND FUTURE WORK

This study presents a novel soft contact pad with five types of embedded sensors (two tactile, one acoustic, one capacitive one temperature, and one accelerometer) and a high-accuracy terrain classification algorithm, which opens the opportunity for our Cassie robot to identify the terrain and design terrain-aware planning and control. The elastomeric pad encapsulates and protects the sensors, and also serves to tune the force range of the tactile sensor through spatial force distribution. The sensorized foot was attached to an Instron and put through cyclic impact motions to model the stepping behavior of the Cassie robot. The impact data was put through a feature-based classification algorithm that combines Random Forests with designed memory function. The result of cross-validation shows the algorithm has a high classification accuracy as 96.5%. Furthermore, different comparisons are conducted, showing the redundancy of integrated sensors and the robustness of our trained model.

We are extensively evaluating various real-world terrains under harsh conditions, in particular, improving our current classification algorithms to handle terrains composed of a mixture of two or three types of granular media considered in this study. Also, when a sensor failure occurs, a switching mechanism of classification algorithms is essential to accommodate this emergency situation.

Meanwhile, we will extract and represent patch contact forces from the tactile sensor. Accordingly, both classified terrain information and contact forces will be encoded as symbolic representations and incorporated into the Cassie locomotion planning and control optimization algorithms. The long-term goal is to enable Cassie for real-time terrain-aware maneuvering over highly rough terrain.

REFERENCES

- [1] K. Walas, "Terrain classification and negotiation with a walking robot," *Journal of Intelligent & Robotic Systems*, vol. 78, no. 3-4, pp. 401–423, 2015.
- [2] X. D. A. H. O. H. J.-K. H. Yukai Gong, Ross Hartley and J. Grizzle, "Feedback control of a cassie bipedal robot: Walking, standing, and riding a segway," in *2019 American Control Conference (ACC)*. IEEE, 2019, pp. 4559–4566.
- [3] J. Christie and N. Kottege, "Acoustics based terrain classification for legged robots," in *2016 IEEE International Conference on Robotics and Automation (ICRA)*. IEEE, 2016, pp. 3596–3603.
- [4] J. Aguilar, T. Zhang, F. Qian, M. Kingsbury, B. McInroe, N. Mazouchova, C. Li, R. Maladen, C. Gong, and M. Travers, "A review on locomotion robophysics: the study of movement at the intersection of robotics, soft matter and dynamical systems." *Reports on Progress in Physics Physical Society*, vol. 79, no. 11, p. 110001.
- [5] X. Xiong, A. D. Ames, and D. I. Goldman, "A stability region criterion for flat-footed bipedal walking on deformable granular terrain," in *2017 IEEE/RSJ International Conference on Intelligent Robots and Systems (IROS)*. IEEE, 2017, pp. 4552–4559.
- [6] C. M. Hubicki, J. J. Aguilar, D. I. Goldman, and A. D. Ames, "Tractable terrain-aware motion planning on granular media: an impulsive jumping study," in *2016 IEEE/RSJ International Conference on Intelligent Robots and Systems (IROS)*. IEEE, 2016, pp. 3887–3892.
- [7] L. Wagner, P. Fankhauser, M. Bloesch, and M. Hutter, "Foot contact estimation for legged robots in rough terrain," in *Advances in Cooperative Robotics*. World Scientific, 2017, pp. 395–403.
- [8] J. R. Rebula, P. D. Neuhaus, B. V. Bonnlander, M. J. Johnson, and J. E. Pratt, "A controller for the littledog quadruped walking on rough terrain," in *Proceedings 2007 IEEE International Conference on Robotics and Automation*. IEEE, 2007, pp. 1467–1473.
- [9] S. Zenker, E. E. Aksoy, D. Goldschmidt, F. Wörgötter, and P. Manoonpong, "Visual terrain classification for selecting energy efficient gaits of a hexapod robot," in *2013 IEEE/ASME International Conference on Advanced Intelligent Mechatronics*. IEEE, 2013, pp. 577–584.
- [10] J. Mrva and J. Faigl, "Feature extraction for terrain classification with crawling robots." in *ITAT*, 2015, pp. 179–185.
- [11] J. Libby and A. J. Stentz, "Using sound to classify vehicle-terrain interactions in outdoor environments," in *2012 IEEE International Conference on Robotics and Automation*. IEEE, 2012, pp. 3559–3566.
- [12] P. Giguere and G. Dudek, "A simple tactile probe for surface identification by mobile robots," *IEEE Transactions on Robotics*, vol. 27, no. 3, pp. 534–544, 2011.
- [13] ———, "Surface identification using simple contact dynamics for mobile robots," in *2009 IEEE International Conference on Robotics and Automation*. IEEE, 2009, pp. 3301–3306.
- [14] P. Dallaire, K. Walas, P. Giguere, and B. Chaib-draa, "Learning terrain types with the pitman-yor process mixtures of gaussians for a legged robot," in *2015 IEEE/RSJ International Conference on Intelligent Robots and Systems (IROS)*. IEEE, 2015, pp. 3457–3463.
- [15] J. J. Shill, E. G. Collins, E. Coyle, and J. Clark, "Terrain identification on a one-legged hopping robot using high-resolution pressure images," in *2014 IEEE International Conference on Robotics and Automation (ICRA)*. IEEE, 2014, pp. 4723–4728.
- [16] X. A. Wu, T. M. Huh, R. Mukherjee, and M. Cutkosky, "Integrated ground reaction force sensing and terrain classification for small legged robots," *IEEE Robotics and Automation Letters*, vol. 1, no. 2, pp. 1125–1132, 2016.
- [17] H. Kolvenbach, C. Bärtschi, L. Wellhausen, R. Grandia, and M. Hutter, "Haptic inspection of planetary soils with legged robots," *IEEE Robotics and Automation Letters*, vol. 4, no. 2, pp. 1626–1632, 2019.
- [18] P. Giguere, G. Dudek, S. Saunderson, and C. Prahalas, "Environment identification for a running robot using inertial and actuator cues." in *Robotics: Science and Systems*, 2006.
- [19] F. L. G. Bermudez, R. C. Julian, D. W. Haldane, P. Abbeel, and R. S. Fearing, "Performance analysis and terrain classification for a legged robot over rough terrain," in *2012 IEEE/RSJ International Conference on Intelligent Robots and Systems*. IEEE, 2012, pp. 513–519.
- [20] J. Degrave, R. Van Cauwenbergh, F. Wyffels, T. Waegeman, and B. Schrauwen, "Terrain classification for a quadruped robot," in *2013 12th International Conference on Machine Learning and Applications*, vol. 1. IEEE, 2013, pp. 185–190.
- [21] I. Halatci, C. A. Brooks, and K. Iagnemma, "A study of visual and tactile terrain classification and classifier fusion for planetary exploration rovers," *Robotica*, vol. 26, no. 6, pp. 767–779, 2008.
- [22] R. J. Kate, "Using dynamic time warping distances as features for improved time series classification," *Data Mining and Knowledge Discovery*, vol. 30, no. 2, pp. 283–312, 2016.
- [23] M. C. Ozkul, A. Saranli, and Y. Yazicioglu, "Acoustic surface perception from naturally occurring step sounds of a dexterous hexapod robot," *Mechanical Systems and Signal Processing*, vol. 40, no. 1, pp. 178–193, 2013.
- [24] L. Breiman, "Random forests," *Machine learning*, vol. 45, no. 1, pp. 5–32, 2001.
- [25] C.-C. Chang and C.-J. Lin, "LIBSVM: A library for support vector machines," *ACM Transactions on Intelligent Systems and Technology*, vol. 2, pp. 27:1–27:27, 2011, software available at <http://www.csie.ntu.edu.tw/~cjlin/libsvm>.